Status of the Slip Stacking Beam Studies

Kiyomi Koba

June 7, 2003

Abstract

We have started beam studies for 'slip stacking'[1][2][3][4] in Main Injector(MI) in order to increase proton intensity for anti-proton production.[5][6][7] It has been verified that the system for slip stacking works for a low intensity beam. No unpredictable emittance blow up was observed and the beam was accelerated to 120GeV with 98% efficiency. For high intensity operation, development work of the feedback and feed-forward systems is under way[8][9][10].

1. Introduction

For slip stacking, we use three different rf systems and follow four steps. Step 1: The first bunch train is injected from the Booster on the central orbit and captured by the first rf system. To make a room for the second bunch train, the first bunch train is then decelerated until it circulates on the inside of the central orbit. Step 2: The second bunch train is injected on the central orbit and captured by the second rf system. Step 3: As the two bunch trains have slightly different energies, they can move relative to each other. Step 4: When the two bunch trains coincide at the same longitudinal location, they are captured by the third rf system.

Beam studies of the slip stacking process have started and we have already established that the stacking procedure works as expected. Frequency separation and Booster bunch rotation studies were also done to allow us minimize the longitudinal emittance at recapture. Beam was also accelerated to 120GeV.

2. Momentum aperture scan

Since two bunch trains have different energies, MI must have an enough momentum aperture to accept both. The momentum aperture of MI is +/-0.7% at injection, Fig. 1, corresponding to the frequency separation of +/-3000Hz from the central value of 52.8114MHz.

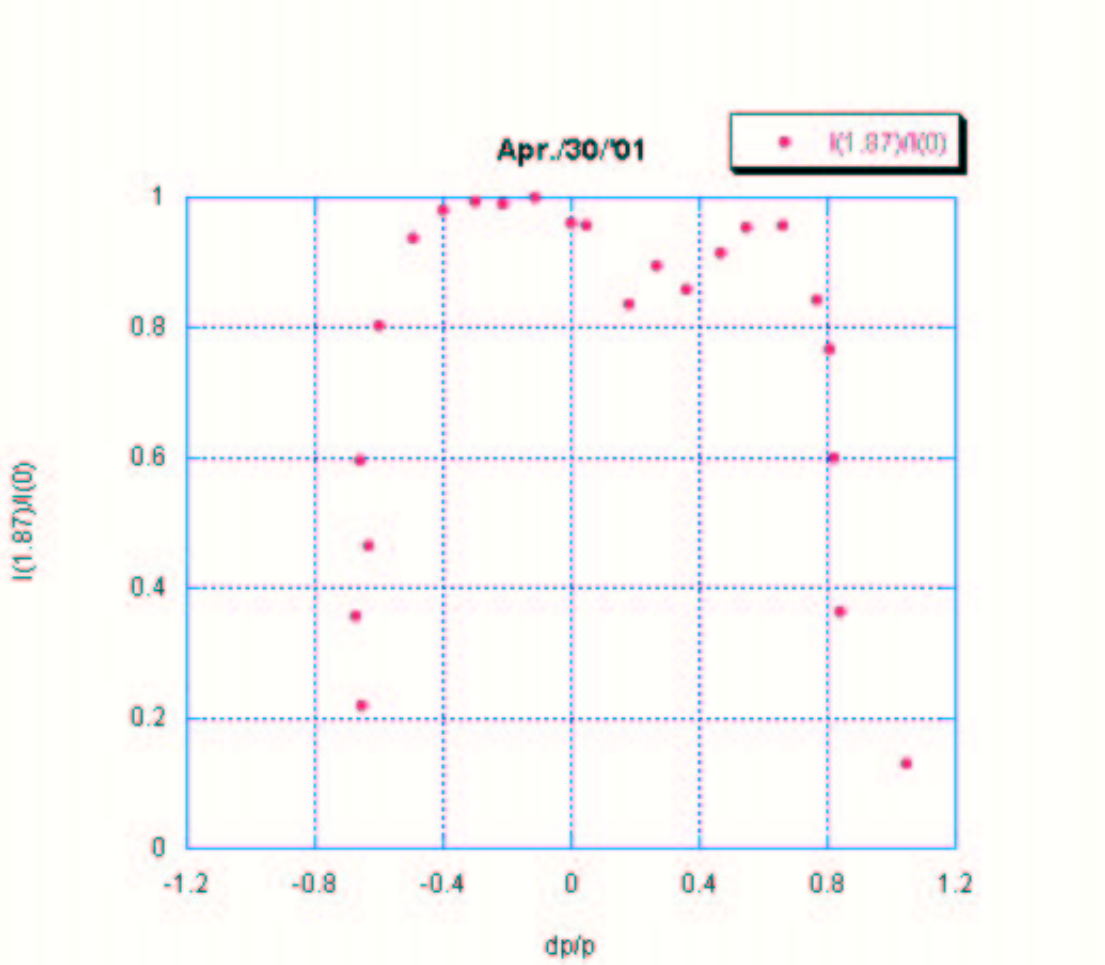

Figure 1. Momentum aperture scan at MI injection. Beam loss ratio as a function of momentum spread.

3. Frequency separation

Since there are two rf voltages during stacking, they act on both bunch trains. The bunch shape has been measured to demonstrate that the frequency separation between the first and the second rf systems is adequate.

In this measurement, one bunch train was injected, then two rf voltages were raised and the frequency separation was increased from 400 to 1200Hz. Figure 2 shows the bunch shape at injection and at 150msec after injection. The signals, plotted here with 5nsec/div, were obtained with a wall current monitor. It is clear that the frequency separation of 1200Hz is enough to keep the bunch shape unchanged.

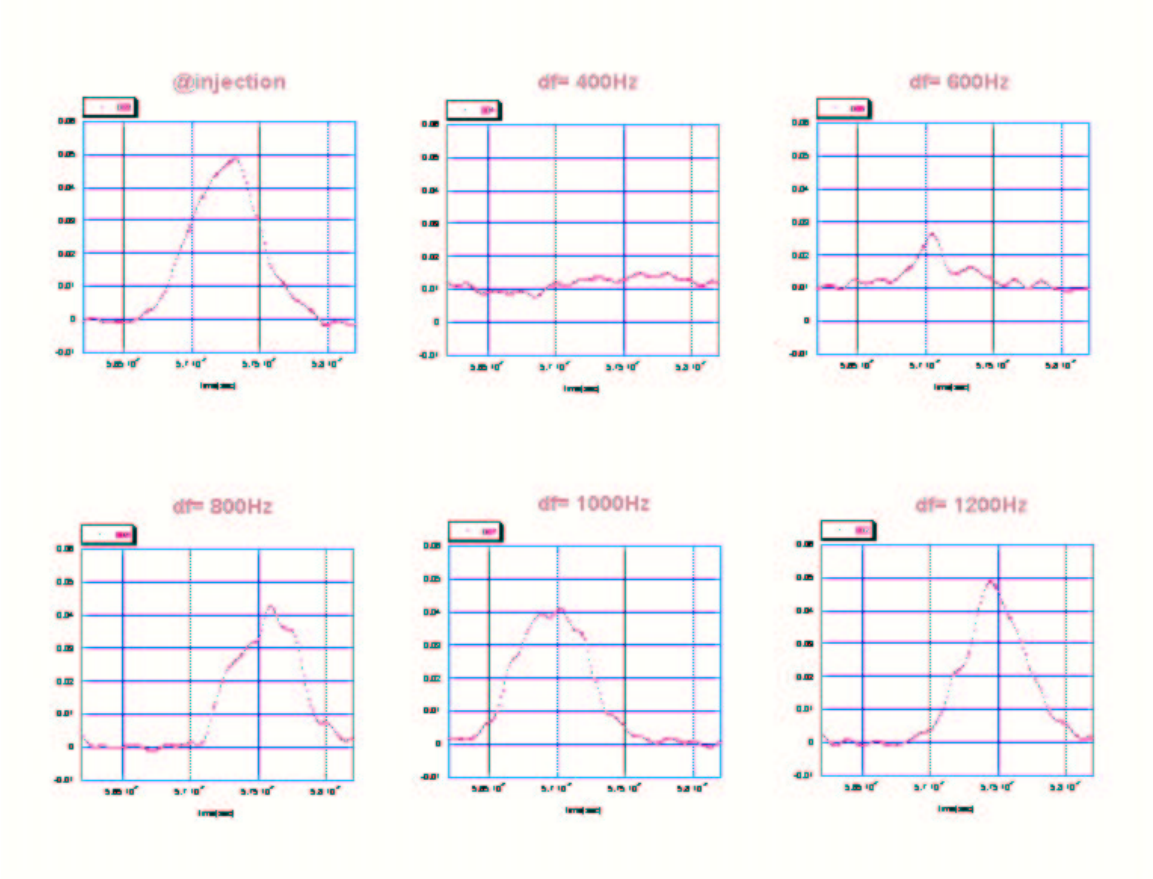

Figure 2. Wall current monitor signals at injection and after 0.15msec.

4. RF system

MI has 18 53MHz cavities. These are in to two groups, A and B, each with 9 cavities. Low level RF (LLRF) signals go to two groups of cavities individually. For the slip stacking, we are using one out of 9 cavities in each group at injection. The rf voltage at injection is adjusted so that one cavity produces 62 kV in order to achieve a low momentum spread.

5. Injection matching from Booster to MI

At extraction, the Booster rf voltage is 380kV, which matches to MI injection voltage of 1MV for the normal operation. Since the MI injection rf voltage is 62 kV for the slip stacking, a bunch rotation is carried out in Booster before extraction so that the bunch shape will be matched to the rf bucket of MI at injection. As the Booster rf voltage is rapidly reduced, the bunch starts to rotate in the phase space. After a quarter of synchrotron period, the bunch is injected to MI. Figure 4 shows the wall current monitor (WCM) signal at Booster extraction. The rf voltage was changed from 380kV to 130kV in 50μsec and the bunch started a rotation with the rotation period of ~300μsec.

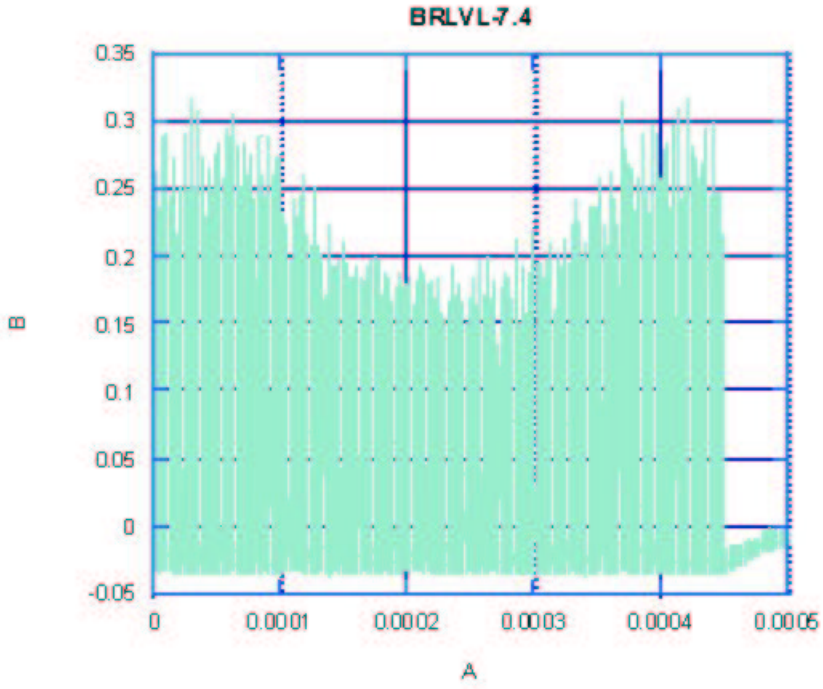

Figure 3. Bunch rotation process at Booster extraction. WCM voltage as a function of time.Horizontal scale is 100μsec/div.

6. RF frequency curves

The frequency as a function of time is shown in Figure 4 for the first and the second rf systems. Of 18 cavities at 53MHz, one was used for the first system, another for the second system. The frequency separation was kept at 1200Hz. The first bunch train was injected on the central orbit with nominal frequency at 0.13msec and captured by the first rf system of 62kV. At this time, the frequency of the second rf system was 1200Hz higher than the first rf system. The first bunch was then decelerated to the frequency 1200Hz lower than the original value. After one Booster cycle of 66.7msec, the second train was injected on the central orbit and captured by the second rf system. After slipping, both bunch trains were captured by all 18 cavities with 800kV and 0 frequency separation.

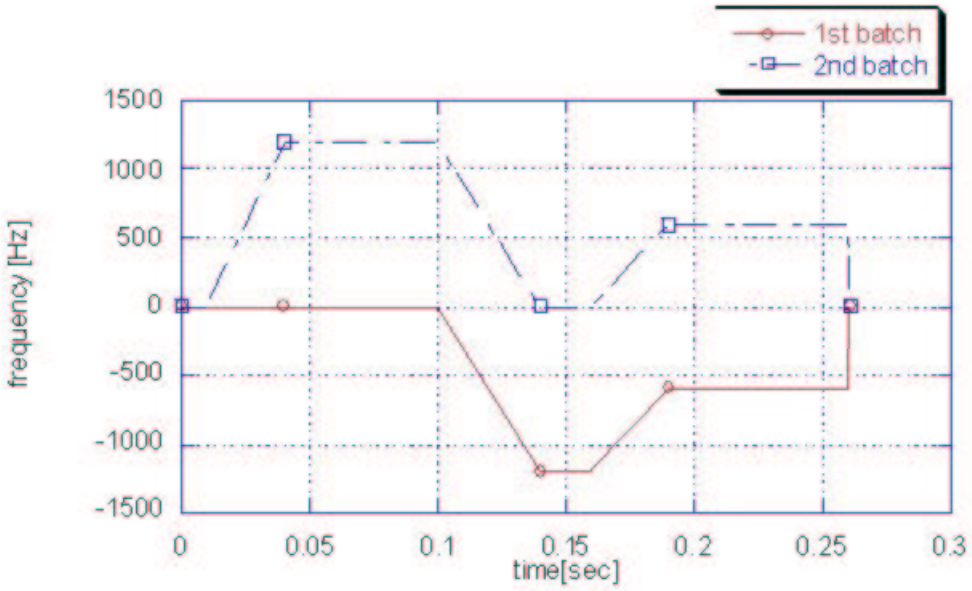

Figure 4. Frequency for 1st bunch train and 2nd bunch train as a function of time.

7. Early beam studies

Two bunch trains, each with 82 bunches, were injected to MI. The total intensity for two trains was low, $0.8*10^{12}$ppp, in order to reduce beam loading effects.

Figure 5, a mountain range picture of the signals from the WCM, reveals the progress of slip stacking from the beginning to the end. The signal came from WCM with a resolution of 0.5nsec/sample. The data were obtained every 1.42msec for 0.18sec. At the same time, the total beam-intensity and the intensity within the gate equivalent to one rf bucket width were also measured and plotted in Fig.6. The one bucket intensity was 9E9 which is equal to 0.8E12/(82*2). This indicates that there was no beam loss during the slip stacking process. The intensity of the 1st bunch of the1st bunch train was estimated by integration of bunch area obtained by the WCM. Figure 7 shows the result of the integration and the position of the center of the bunch. When two bunches were recaptured by one rf bucket after 0.17 sec, the intensity became twice of what was before while the bunch position did not move.

The length of the first bunch of the first bunch train shown in Fig. 5 was used to calculate the emittance. Figure 8 shows the calculated 95% emittance during 0.18s. Since there was an empty space between upper and lower bunches, there should be an emittance

growth. The emittance growth expected from simulation is a factor of 3.2. From the plot, we see that there is no emittance growth before the two batches are recaptured by one RF bucket but there is a factor of 4.0 emittance growth after the recapture.

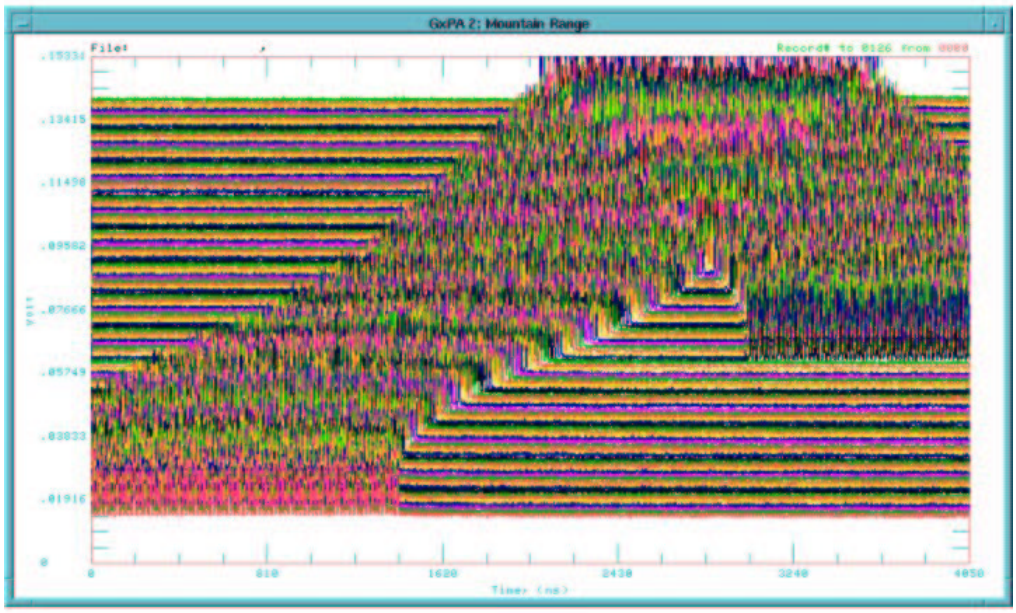

Figure 5. Mt range plot. The signal came from WCM with a resolution of 0.5ns/sample. The data were obtained every 1.42ms for 0.18s.

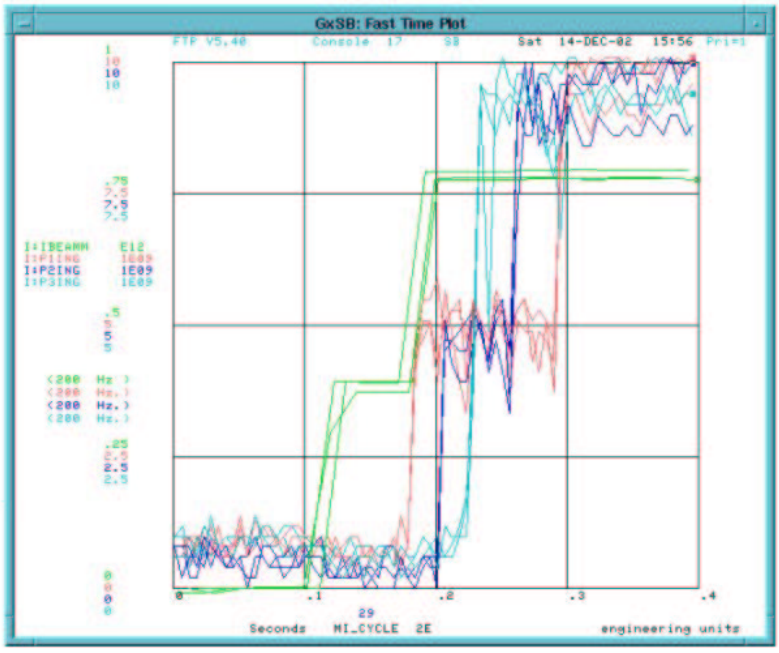

Figure 6. Total beam-intensity(I:BEAMM) and the intensity within the gate equivalent to one RF bucket width at 2000nsec(I:P1ING), 2400nsec(I:P2ING) and 2800nsec(I:P3ING).

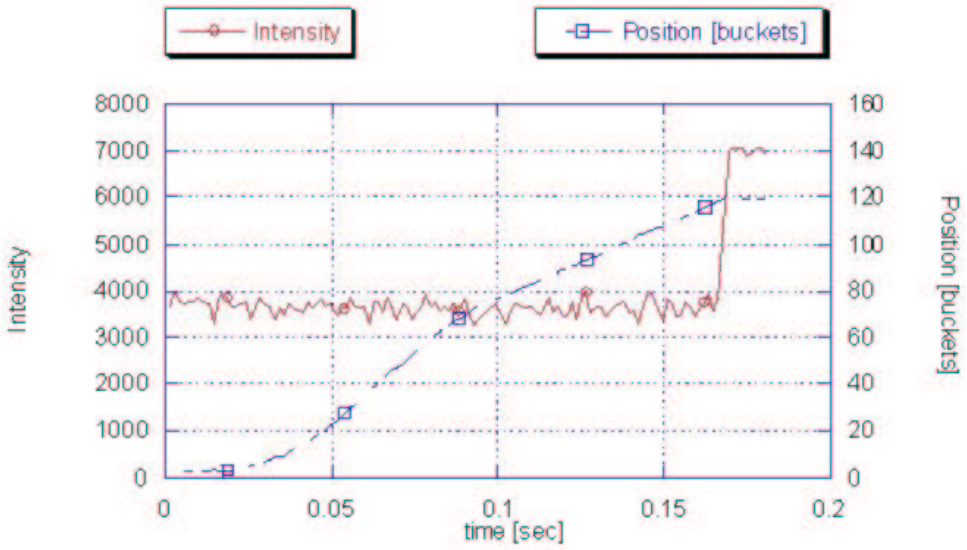

Figure 7. The intensity of the 1st bunch of the1st bunch train was estimated by integration of bunch area shown in Fig.5. The center position of the bunch was also measured.

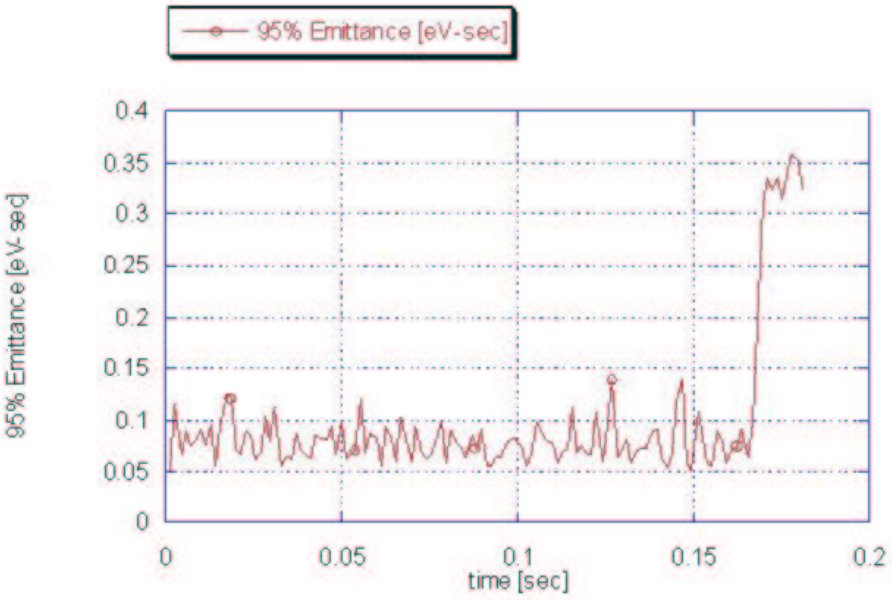

Figure 8. The 95% emittancecalculated by bunch length shown in Fig.5.

9. Slip stacking phase variation and LLRF improvements

Frequency curves (Fig.4) applied to the beam are calculated assuming that, at the time of recapture, two bunch trains are sitting exactly on the same longitudinal location, that is, two cavities are in phase. However, MI slip stacking studies revealed cycle to cycle variation in the RF system phase slip as shown in Fig. 9. This produced an unreliable RF voltage for recapture.

The largest phase variation was traced to timing jitter on the 720Hz line locked Tevatron Clock event. A MI LLRF system Digital Signal Processor (DSP) generates the frequency curves from user tuned tables. The frequency curves are a function of time and are integrated by the DSP to apply phase modulation to the RF systems that slip the bunch trains. The DSP processes run at 720Hz, 23*720Hz, and 138*720Hz via a scheduler that is synchronized with the Tevatron Clock event by a phase lock loop (PLL). As the PLL input jitters and the DSP follows the jitter, the frequency curves output and its integral (RF phase) varies.

The RF phase variation was reduced to 0° from 45° which was causing time jitter of 200μsec, by changing the frequency curve generation from the Tevatron Clock time base to accurate LLRF internal time(Fig. 10).

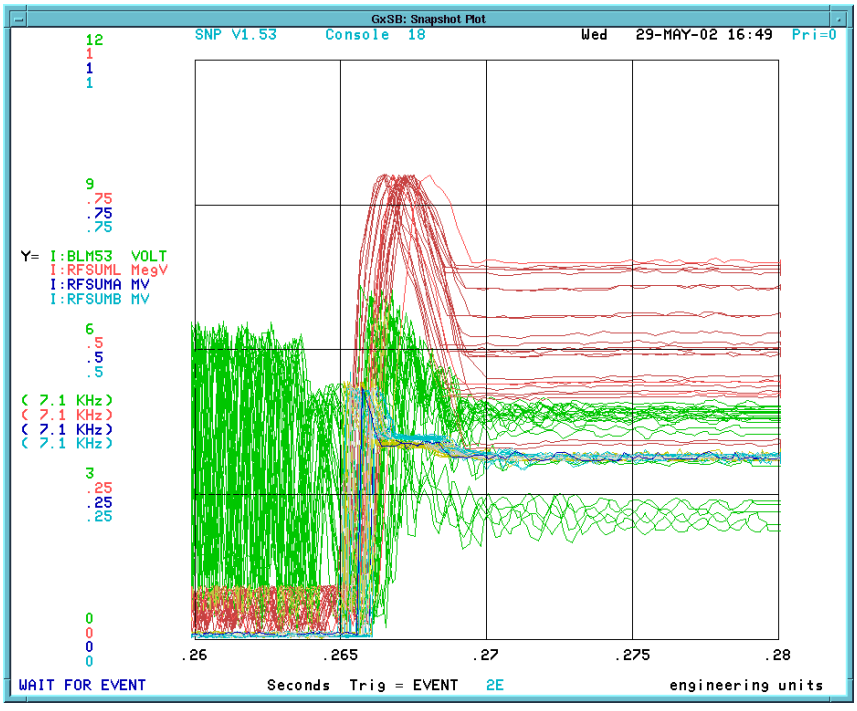

Figure 9. RF voltage(I:RFSUML) around the recapture time before LLRF timing jitter was fixed.

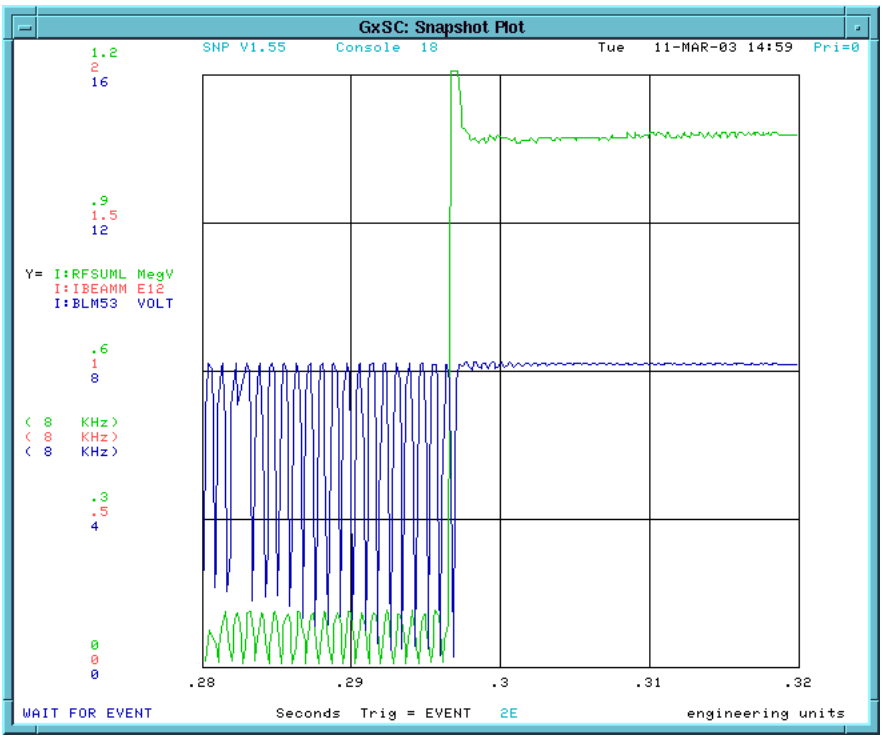

Figure 10. RF voltage(I:RFSUML) around the recapture time after LLRF timing jitter was fixed.

9. Simulation studies

To understand what caused the emittance growth at recapture, simulation studies were carried out using the code ESME[11]. In the simulation studies, the time and amplitude of the voltage to recapture bunches were varied to match the observed RF phase and amplitude variation as shown in Fig. 9.

Figure 11 shows the phase space at recapture time. The delay was changed from 0 to 250 μsec causing a +/-60 degrees phase variation and the 95% bunch length after 15msec was measured. The emittance plotted in Fig. 12 was estimated from the bunch length. It increased by a factor of 3.2 to 7.0 with increasing delay. Since the RF phase variation produced errors as large as 45 degrees, it could cause the emittance growth.

The recapture voltage was changed from 0.5 to 1.0MV because the voltage is changing from 0.8 to 1.0MV after the time to recapture. The 95% emittance plotted in Fig. 13 shows the emittance growth by a factor of 3.2 to 3.6.

By the two simulation studies, it was verified that the emittance growth is mainly due to time jitter.

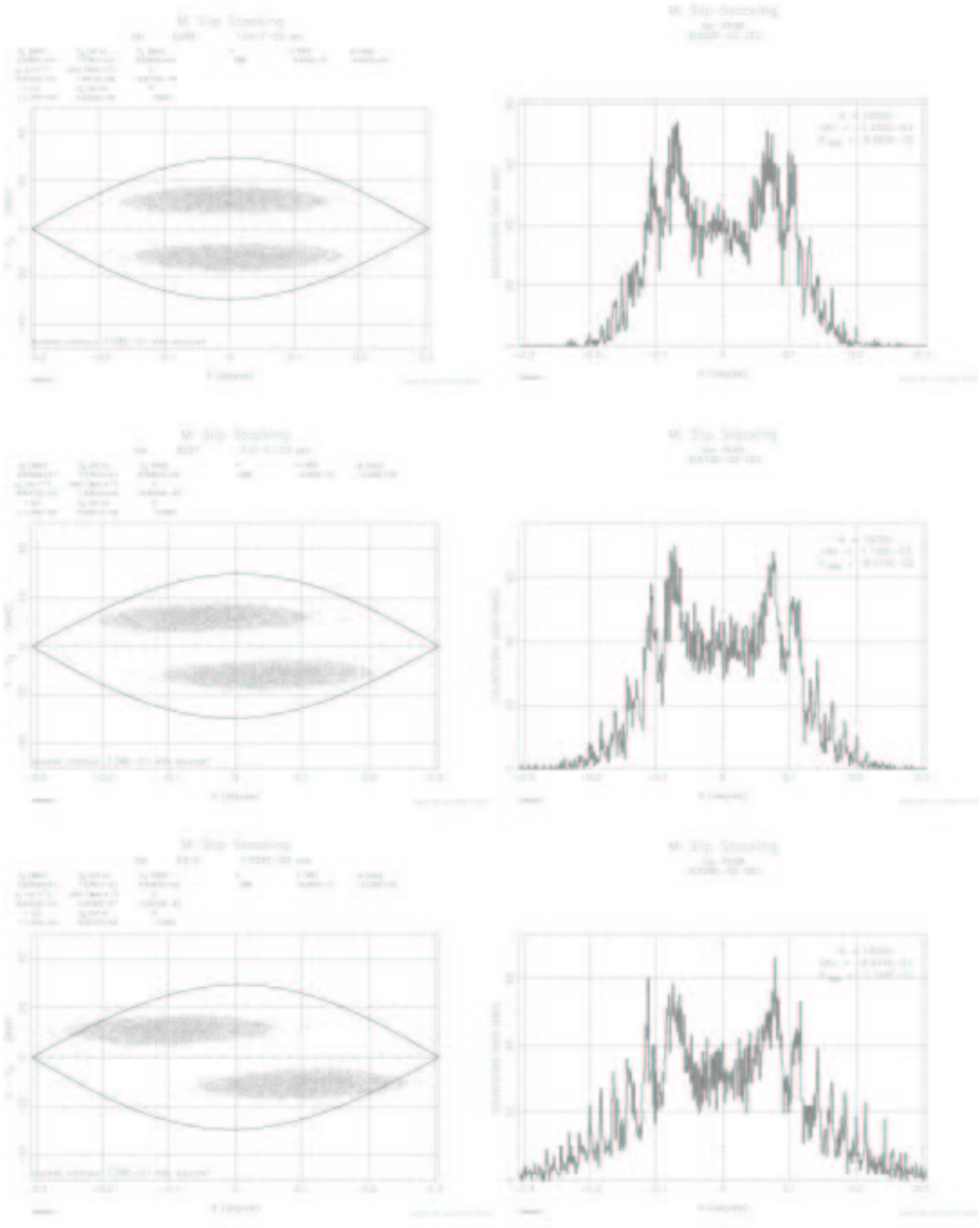

Figure 11. The phase space at recapture time and bunch shape after 15msec. The delay were 0sec(upper), 100μsec(middle) and 250 μsec(lower).

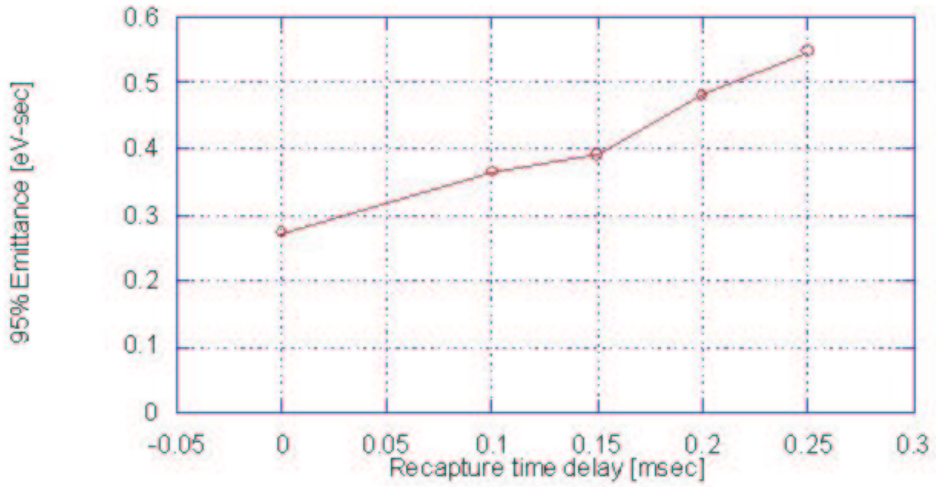

Figure 12. The 95% emittance estimated VS recapture delay time.

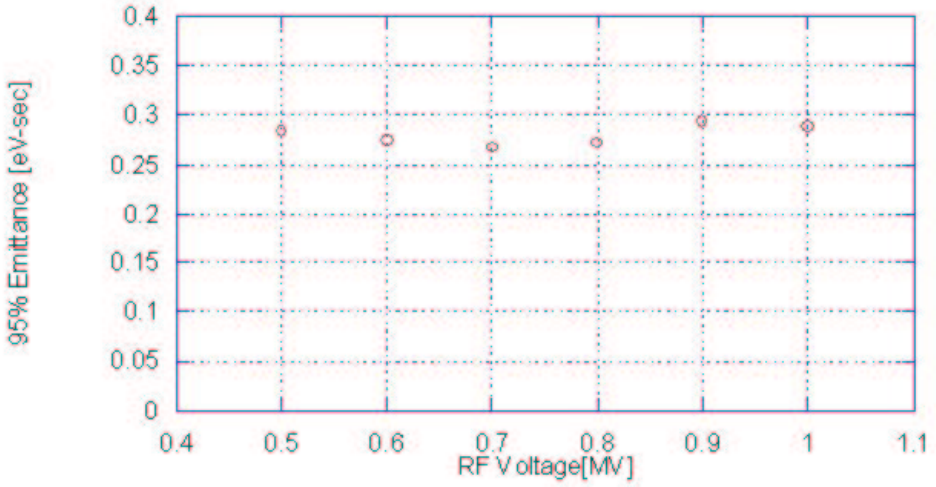

Figure 13. The 95% emittance estimated VS recapture rf voltage.

10. Latest Beam Studies and Emittance measurements

The low intensity slip stacking studies were repeated after the LLRF improvements. Figure 14, a mountain range picture, shows the progress of slip stacking around recapture time. The signal comes from a wall current monitor (WCM) with a resolution of 0.5nsec/sample. Upper picture was taken with time jitter and lower picture after the improvement. The bunch width is now narrower than before.

The 95 % longitudinal emittance was measured again during 0.18sec and this was compared with the previous one and plotted in Fig. 15. A factor of 3.2 in the observed emittance growth rate is the same as simulation results and there is no unexpected emittance growth during slip stacking.

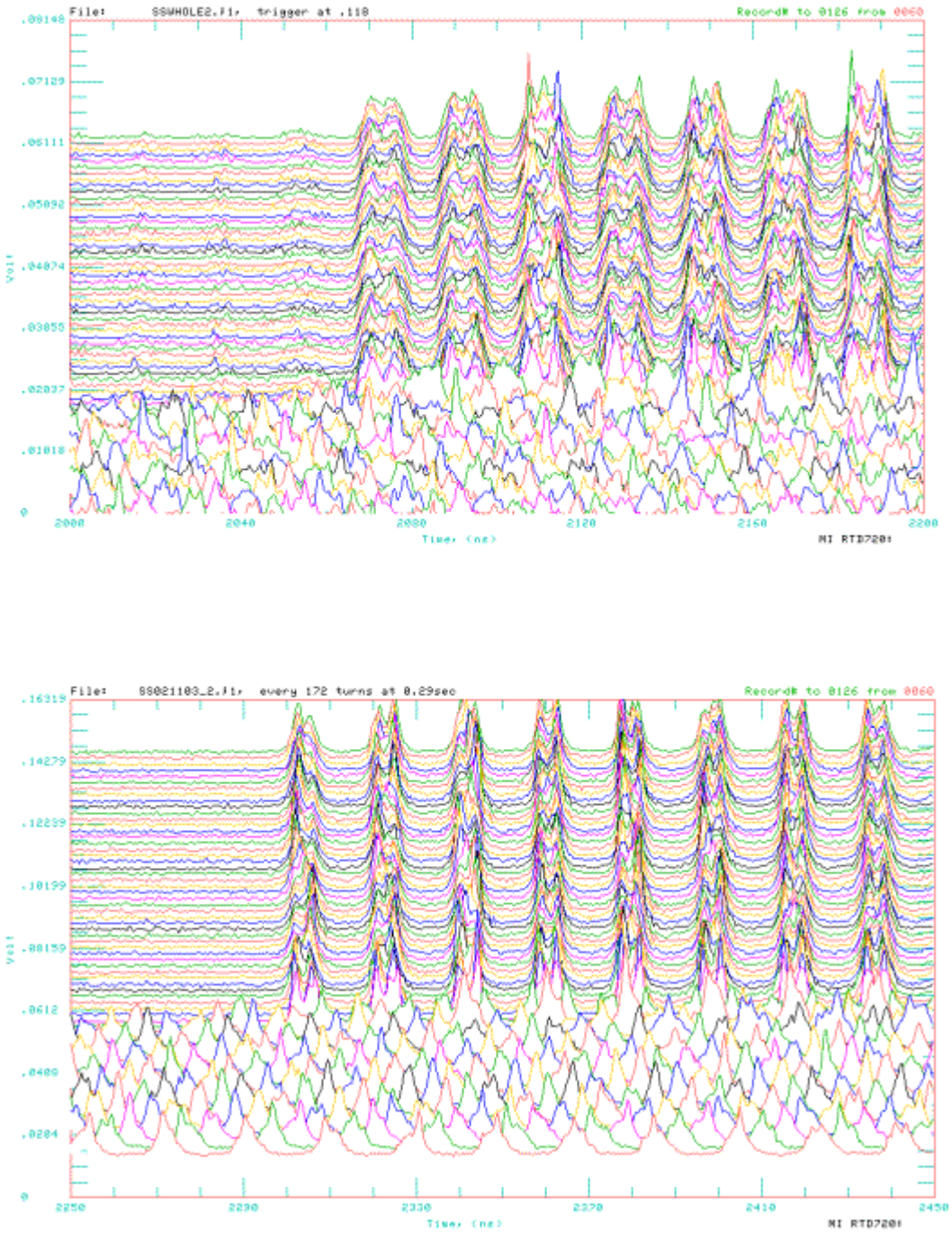

Figure 14. Mountain range plots of wall current monitor signals around recapture time. Upper: before the LLRF improvements. Lower: after the LLRF improvements.

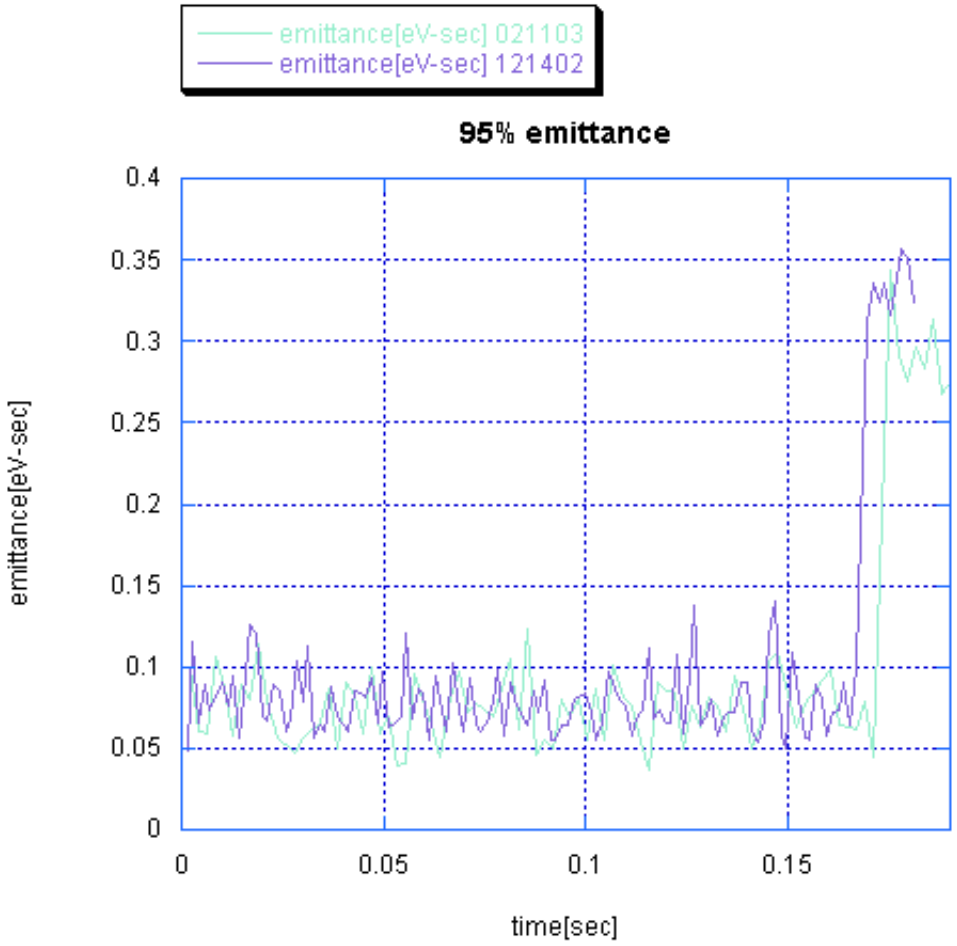

Figure 15. Comparison of the emittance before and after the LLRF improvements. Blue trace: before the improvements. Green trace: after the improvements.

11. Acceleration

Acceleration was also tried. Figure 16 shows the beam intensity during beam acceleration. Approximately 1.0E12 total particles were injected, slip stacked and accelerated to 120GeV. There was a beam loss of ~2% at the beginning of acceleration.

The emittance at 120GeV was measured and plotted in Fig. 17. The observed value of 0.24eV-sec is less than that the one we currently have in the normal operation cycle.

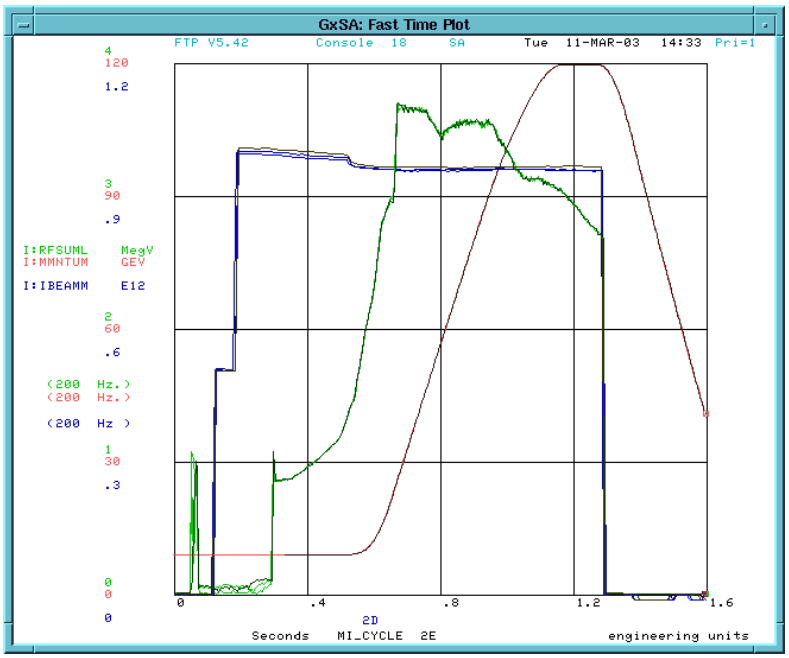

Figure 16. RFSUML: rf voltage[MV], MMNTUM: momentum[GeV], IBEMM: total beam intensity [E12 ppp]

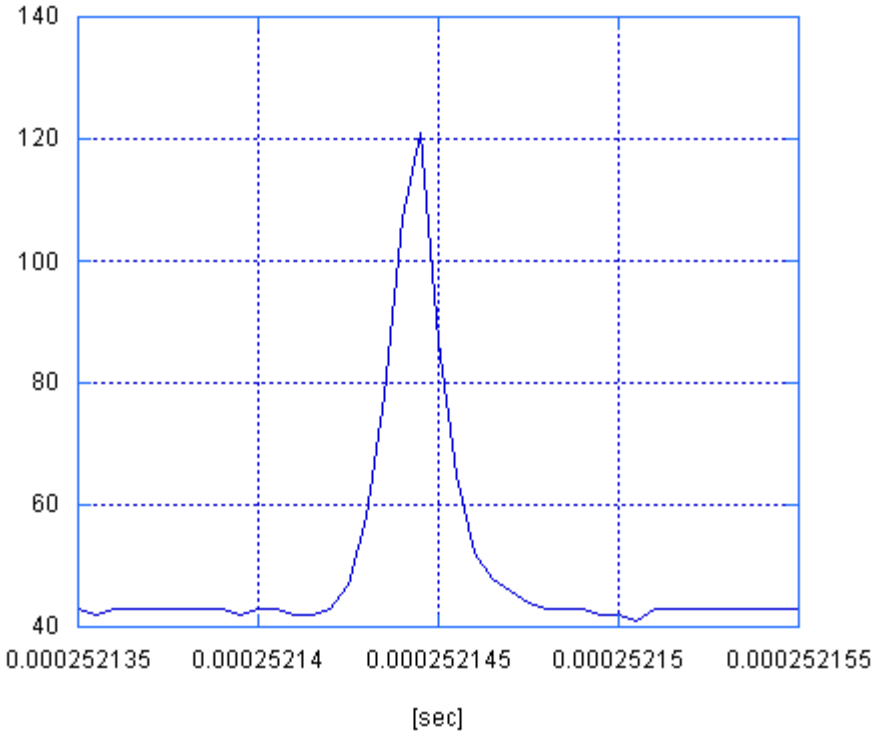

Figure 17. Bunch shape at 120GeV. 5nsec/div.

12. Conclusion

Beam studies have stared for the slip stacking process, and we have already verified that, at least for low beam intensity, the stacking procedure works as expected.

There was no beam loss during the process, but there was emittance growth when two bunch trains were recaptured. Simulation studies have indicated that the emittance growth is caused by RF phase variation.

The RF phase variation was eliminated and the emittance was measured again. No undesirable emittance blow up has been observed.

Beam has been accelerated to 120GeV with a beam loss of ~2% at the beginning of acceleration.

For higher intensity operation, development of the feedback and feed-forward system is under way.

References

[1] D. Boussard and Y. Mizumachi, "Production od Beams with High Line-Density by Azimutial Combination of bunches in a Synchrotron", IEEE Trans. Nucl. Sci., vol./ NS-26, No3, June, 1979

[2] C. Ankenbrandt, "Slip Stacking: A New Method of Momentum Stacking", Fermilab internal note FN-532, 1981

[3] S. Shukla et al, "Slip Stacking in the Fermilab Main Injector.", Snowmass'96, June 1996.

[4] J. A. MacLachlan, "The Beam Dynamics of Slip Stacking", Fermilab FN-0711, November 2001.

[5] K. Koba, "Slip Stacking," ICFA2002, April 2002.

[6] K. Koba," Emittance measurement and acceleration – Revision of MI-0294", MI-0294

[7] K. Koba," Slip Stacking at Low Intensity – Status of the Beam Studies", MI-0296

[8] J.Dey, J. Steimel and J. Reid, "Narrowband Beam Loading Compensation in the Fermilab Main Injector Accelerating Cavities", 2001 PAC, p. 876, Chicago, June 2001.

[9] J. Dey, et al, "53 MHz Feedforward Beam Loading Compensation in the Fermilab Main Injector," PAC '03.

[10] J. Steimel et al," Beam Loading Compensation for Slip Stacking", PAC '03.

[11] J. A. MacLachlan, "Users Guide to ESME", 2002

.